Slovak University of Technology in Bratislava
Institute of Information Engineering, Automation, and Mathematics

PROCEEDINGS

of the 18th International Conference on Process Control

Hotel Titris, Tatranská Lomnica, Slovakia, June 14 – 17, 2011

ISBN 978-80-227-3517-9

http://www.kirp.chtf.stuba.sk/pc11

Editors: M. Fikar and M. Kvasnica

Sivalingam, S., Hovd, M.: Use of Cross Wavelet Transform for Diagnosis of Oscillations Due to Multiple Sources, Editors: Fikar, M., Kvasnica, M., In *Proceedings of the 18th International Conference on Process Control*, Tatranská Lomnica, Slovakia, 443–451, 2011.

Full paper online: http://www.kirp.chtf.stuba.sk/pc11/data/abstracts/015.html

Use of cross wavelet transform for diagnosis of oscillations due to multiple sources

Selvanathan Sivalingam * **Morten Hovd** **

* *Engineering Cybernetics Department, NTNU, Trondheim 7491, Norway (e-mail: selvanat@itk.ntnu.no)*
** *Engineering Cybernetics Department, NTNU, Trondheim 7491, Norway (e-mail: morten.hovd@itk.ntnu.no)*

Abstract: Oscillations are the most prominent indications of deteriorated controller performance. Control loop oscillations are a common type of plant-wide disturbance and the root-causes can be one or more among poorly tuned controllers, process or actuator non-linearities, presence of model plant mismatch and oscillatory disturbances. This article addresses detection and diagnosis of oscillations in measurements due to multiple sources under a framework of internal model control. A pattern recognition based approach using cross wavelet transforms is proposed to pinpoint the source(s) of oscillation in the control loops. The phase information in wavelet domain between input and output signals is exploited to diagnose the source(s) of oscillations.

Keywords: wavelet transform, oscillation, valve stiction, phase, pattern recognition

1. INTRODUCTION

It is well known that performance degradation in control loops manifests as one or more of the following: (*i*) poor set point (SP) tracking (*ii*) oscillations (*iii*) poor disturbance rejection and (*iv*) excessive final control element variation. Oscillations are attributed to one or more among poor controller tuning, process or actuator non-linearities, presence of model plant mismatch or oscillatory disturbances. A tool to help the engineer should therefore automatically bring oscillatory loops to his or her attention, characterize them and highlight the presence of plant wide oscillations. Several authors have addressed the detection of oscillatory measurements in process data. Early works appear in Hägglund (1995) followed by (Thornhill and Hägglund 1997, Forsman and Stattin 1999, Rengaswamy *et al.* 2001, Tangirala *et al.* 2007). Hägglund (1995) proposed a technique to detect oscillating loops "on-line" using the IAE criterion. This method does not assume any particular shape for oscillation and only requires the measurement to deviate significantly from the set point. Hägglund (1995) also proposed a diagnostic procedure for finding the source of oscillation and eliminating it. The diagnostic procedure is carried out by disconnecting the feedback (*i.e.* switching the controller to manual mode). This approach is simple and efficient and probably the most comprehensive procedure available for diagnosing root cause for oscillations. However, switching the controller to manual mode may not always be allowed, especially if the loop is deemed critical. Further, it will not be possible to apply this approach on thousands of loops in a routine fashion. Thornhill and Hägglund (1997) presented an offline technique for detecting oscillation using a regularity factor. This method requires the user to specify the root-mean-square value of the noise and a thresholds a nontrivial task when applied to hundreds of loops.

Thornhill and Hägglund (1997) and Thornhill *et al.* (2003) proposed a set of procedures to detect and diagnose oscillating loops using offline data. They combine the techniques of controller performance assessment along with operational signatures (OP-PV plots) and spectral analysis of the controller error for diagnosis. This technique, though not completely automated, can distinguish the cause of oscillation as one of the following: (*i*) poor tuning (*ii*) nonlinearity or (*iii*) external disturbance. However, the downside lies in manually inferring the loop signatures that are based on spectral analysis or on a map of controller output (OP) versus process variable (PV) and isolating the oscillating portion from the entire data. Horch (1999) presented a simple, practical approach to distinguish oscillating loops that are caused by external disturbances and static friction. This approach is based on cross-correlation between the controller output (OP) and process output (PV). The cross-correlation technique failed when the data had intermittent oscillations and the set-point was also changing. Horch and Isaksson (1998) also proposed a technique to identify stiction using nonlinear filters. The method assumed that information such as mass of stem, diaphragm area, and so on for each valve is readily available. Since in a typical process industry facility there can be thousands of control loops, it may be nearly impossible to build/maintain a knowledge base of control valves, making this technique difficult to implement.

Choudhury *et al.* (2004) used higher order statistics for detecting nonlinearity in data and have extended the method for diagnosing stiction by fitting an ellipse of the OP-PV plot and inferring the stiction from an assumed stiction model. The success of this approach lies in correctly identifying the oscillation period and its start and end point in the OP-PV data. Tangirala *et al.* (2007) proposed non-negative matrix factorization for detection and diagnosis of plant-wide oscillations based on source separation

techniques. As can be seen, the task of detecting stiction or other nonlinearities in valves from routine operating data is a challenging task. To summarize, data driven techniques that are presented in the literature till date are useful in (a) assessing the performance of the controller by calculating a figure of merits given that the cause of poor-performance is only due to either an aggressive or sluggishly tuned controller in pure feedback control, (b) detecting oscillating loops with an user-specified parameter, and (c) limited diagnosis of the cause of oscillation based on cross-correlation, power spectral analysis, or OP-PV plots. The current approaches lack (a) the capability to efficiently diagnose oscillations due to multiple sources, (b) the ability to diagnose the causes of time-varying oscillations and (c) an automated means of oscillation diagnosis.

In this work, we have attempted to address some of the aforementioned drawbacks by using wavelet and cross wavelet transforms. This paper is organized as follows: A brief introduction on wavelet transforms is given in Section 2. Problem statement and proposed methodology for an IMC framework are given in Section 3 followed by simulation studies in Section 4. The paper ends with concluding remarks in Section 5.

2. WAVELET ANALYSIS

The main benefit of wavelet analysis over Fourier analysis is that both time and frequency localization can be achieved in the former. This is because wavelet analysis employs a wave packet whereas Fourier analysis uses an infinite wave train of sines and cosines. In recent years, wavelet power transforms have become increasingly popular (Bloomfield *et al.* 2004) while the additionally available phase information has remained untapped.

Wavelet analysis has become a common tool for analyzing localized variations of power within a time series. By decomposing a time series into time–frequency space, one is able to determine both the dominant modes of variability and how those modes vary in time. The wavelet transform can be used to analyze time series that contains varying power at different frequencies. The term "wavelet function" is used generically to refer to either orthogonal or non-orthogonal wavelets. The term "wavelet basis" refers only to an orthogonal set of functions (Torrence and Compo 1998). The use of an orthogonal basis implies the use of the discrete wavelet transform, while a non-orthogonal wavelet function can be used with either the discrete or the continuous wavelet transform. The continuous wavelet transform was developed as an alternative approach to the short-time Fourier transform because the spectrogram is limited in resolution by the extent of the sliding window function. The wavelet analysis is done in a similar way to the short-time fourier transform (STFT) analysis in which the signal is multiplied with a function (*i.e.* the wavelet) similar to the window function in the STFT and the transform is computed separately for different segments of the time-domain signal. However, there are two main differences between the STFT and continuous wavelet transform (CWT). The Fourier transforms of the windowed signals are not taken, and therefore single peak will be seen corresponding to a sinusoid, *i.e.,* negative frequencies are not computed. The width of the window is changed as the transform is computed for every single spectral component, which is the most significant characteristic of the wavelet transform. Throughout this work, we use the standard Morlet wavelet: a Gaussian modulated sine wave of the form (Torrence and Compo 1998)),

$$\psi(\eta) = \pi^{-1/4} e^{i\omega_0 \eta} e^{-\eta^2/2} \tag{1}$$

The quantity $\pi^{-1/4}$ is a normalization factor, $\eta = \frac{n}{s}$ is the dimensionless time parameter, n is the time parameter and s is the scale of the wavelet, $\omega_0 = s\omega$ is the dimensionless frequency parameter and ω is the frequency parameter.

It is to be noted that an infinite number of mother wavelets are available, including the derivative-of-a-Gaussian (DOG) and Paul wavelets. In this work, the complex Morlet wavelet is chosen since it yields a complex wavelet transform, containing information on both amplitude and phase. Since DOG wavelets are entirely real, they may not be used for phase analysis, as their real transforms hold only information on amplitude. Alternatively, the complex Paul wavelet could be employed. However, as the Paul function is more sharply defined in time (in comparison to the more sinusoidal Morlet function), it is better suited for studying pulse-like variations.

2.1 Continuous wavelet transform

The continuous wavelet transform is defined as follows:

$$W(a,\tau) = \frac{1}{\sqrt{a}} \int x(t) \psi^* \frac{(t-\tau)}{a} dt \tag{2}$$

where $\psi(t)$ denotes the mother wavelet. The parameter a represents the scale index which is the reciprocal of frequency and the parameter τ indicates the time shifting (or translation). High scales (low frequencies) correspond to the global information of a signal that usually spans the entire signal, whereas low scales (high frequencies) correspond to detailed information of a hidden pattern in the signal that usually lasts for a relatively shorter time.

The CWT has edge artifacts because the wavelet is not completely localized in time. Cone of Influence (COI) has been defined as the area in which the wavelet power caused by a discontinuity at the edge has dropped by e^{-2} of the value at the edge. Due to the edge effect, confidence limits for the wavelet spectra are required and hence to determine significance levels for wavelet spectra an appropriate background spectrum is required. Red noise spectrum is used as background spectrum and it has the characteristic feature of increasing power with decreasing frequency. In this work, continuous wavelet transform and cross wavelet transform are performed using Morlet wavelet to study the time-frequency properties of the of the output sequences.

2.2 Wavelet scale Vs. Fourier period

The scale can be defined as the distance between oscillations in the wavelet, or it can be some average width of the entire wavelet . The period (or inverse frequency) is the approximate Fourier period that corresponds to the oscillations within the wavelet. For all wavelets, there is

a one-to-one relationship between the scale and period. The relationship can be derived by finding the wavelet transform of a pure cosine wave with a known Fourier period, and then computing the scale at which the wavelet power spectrum reaches its maximum.

For some wavelets the period has more meaning than others. For the Morlet, which has several smooth oscillations, the period is a well-defined quantity which measures the approximate Fourier period of the signal. For the Morlet wavelet , l=1.03a, where l is the Fourier period, indicating that for the Morlet wavelet the wavelet scale (a) is almost equal to the Fourier period.

2.3 Cross-wavelet transform (XWT)

The cross-wavelet transform between two time series X and Y, with wavelet transforms $W_x(f,\tau)$ and $W_y(f,\tau)$ is simply the multiplication of the first complex wavelet transform with the complex conjugate of the second

$$W_{xy}(f,\tau) = W_x(f,\tau)W_y^*(f,\tau) \tag{3}$$

where $f \approx \frac{1}{a}$ when $f_0 = 2\pi$ for the Morlet wavelet. The wavelet scale, a, is inversely proportional to the central frequency of the wavelet (f_o).

While a wavelet power spectrum depicts the variance of a time series with times of large variance showing large power, the cross wavelet power of two time series depicts the covariance between these time series. Additionally, cross wavelet power has a known distribution of confidence levels which is proportional to the square root of the product of two χ^2 distributions (Torrence and Compo 1998). This allows cross wavelet power to be used as a quantified measure of the similarity of power between two time series.

2.4 Phase difference analysis

In complement to wavelet analysis, the phase spectrum analysis can be used to characterize the association between signals. The phase difference provides information on the sign of the relationship (*i.e.,* in phase or out of phase). As the Morlet wavelet is a complex wavelet, the cross wavelet transform relation can be written in terms its modulus $|W_x(f,\tau)|$ and its phase, $\phi_x(f,\tau) = tan^{-1}\frac{\text{Imag}(W_x(f,\tau)}{\text{Real}(W_x(f,\tau)}$. Similarly, with the cross wavelet transform $W_{xy}(f,\tau)$ the phase relation between the time series X and Y can be computed using the relation, $\phi_{xy}(f,\tau) = tan^{-1}\frac{\text{Imag}(W_{xy}(f,\tau)}{\text{Real}(W_{xy}(f,\tau)}$.

The estimation of phase spectrum in Fourier domain between two time series contains relatively large errors compared to that computed in wavelet domain(**?**). Moreover, phase difference is localized in time and frequency in wavelet domain. The arrows in the cross-wavelet transform plot indicate the direction of the phase difference between the variables. The phase arrows pointing right indicate that the variables are in-phase, pointing left indicate the variables are anti-phase, down indicate phase lead of 90° and up refer to phase lag of 90°. The direction of the phase difference between the variables plays a crucial role in diagnosing the source(s) of oscillation in the work.

2.5 Average angle

As we are interested in the phase difference between the components of the two time series, it is necessary to estimate the mean and confidence interval of the phase difference. The circular mean of the phase are used over regions with higher than 5% statistical significance that are outside the COI to quantify the phase relationship. This is a useful and general method for calculating the mean phase. The circular mean of a set of angles (ai , i=1...n) is defined as

$$a_m = \arg(X,Y) \tag{4}$$

with $X = \sum_{i=1}^{n} cos(ai)$ and $Y = \sum_{i=1}^{n} sin(ai)$. It is difficult to calculate the confidence interval of the mean angle reliably since the phase angles are not independent. The number of angles used in the calculation can be set arbitrarily high simply by increasing the scale resolution. However, it is interesting to know the scatter of angles around the mean. For this the circular standard deviation is defined as

$$s = \sqrt{-2\ln\frac{R}{n}} \tag{5}$$

where $R = \sqrt{X^2 + Y^2}$. The circular standard deviation is analogous to the linear standard deviation in that it varies from zero to infinity. It gives similar results to the linear standard deviation when the angles are distributed closely around the mean angle. In some cases there might be reasons for calculating the mean phase angle for each scale, and then the phase angle can be quantified as a number of years. The XWT phase angle within the 5% significant regions and outside the COI has the mean phase 176±12 (where ± designates the circular standard deviation).

3. PROBLEM STATEMENT AND PROPOSED METHOD

Oscillations in model based control loops occur due to either one of (*i*) valve stiction (*ii*) model plant mismatch, (*iii*) external oscillatory disturbances or combination of any of these. It becomes vital to diagnose the causes of oscillations in order to take the appropriate remedial action. A procedure based on pattern recognition techniques using cross wavelet transform is devised in this article to diagnose the cause(s) of the oscillation. The problem is setup in the internal model control (IMC) framework (Figure 1). Cross wavelet transform of input and plant and that of input and model output are computed and thereby a specific pattern is sought for root cause diagnosis of oscillation using the direction of wavelet phase difference between the variables.

To illustrate the idea of cross-wavelet transform for an input-output system, an open-loop process with $G_p(s) = \frac{1}{10s+1}$ is considered. The process is simulated for a sinusoidal input having two frequencies and the time domain plots of input and output are given in Figure 2.

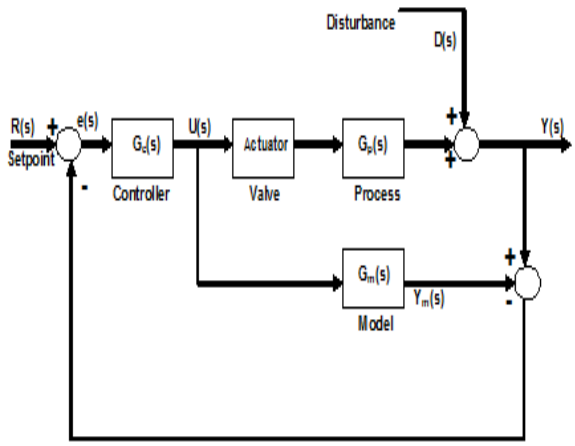

Fig. 1. Schematic representation of internal model control with actuator

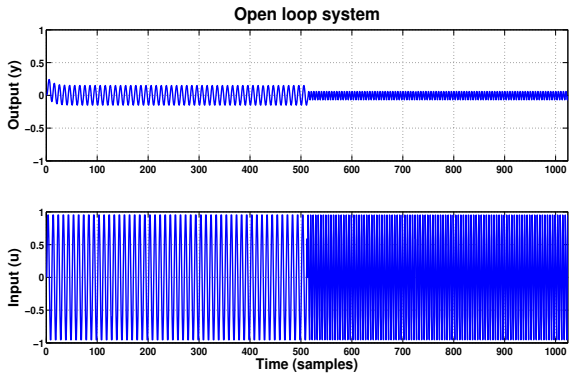

Fig. 2. Time domain behavior of input and output signals considered for interpretation of wavelet analysis

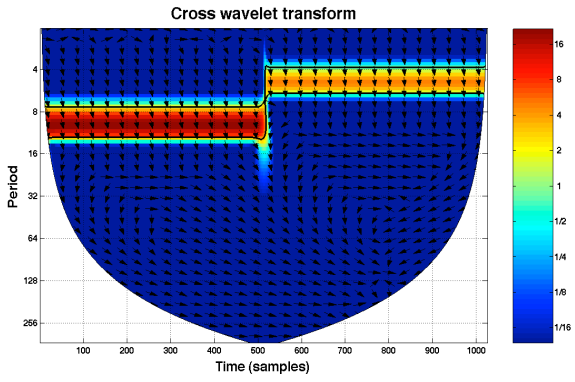

Fig. 3. Cross wavelet transform between input and output signals

The cross wavelet transform plot between two quantities u and y is shown in Figure 3.

It is known from Figure 3 that the quantities u and y show high common power at two frequencies between two different time intervals (0.1 Hz, 0-511 and 0.2 Hz, 512-1024) and the arrows indicate the direction of the wavelet phase between u and y *i.e.,* u leads y by 90° (pointing down). Based on the properties of cross wavelet transform, wavelet phase difference and linear time invariant systems theory, the following methodology is proposed to diagnose the source(s) of oscillation in a control loop.

The quantities controller output (u), process output (y) and model output (y_m) of an oscillating control loop are obtained either from simulation or from industry. The cross wavelet transforms, $W_{uy}(f,\tau)$ and $W_{uy_m}(f,\tau)$ are computed. By comparing the direction of wavelet phase, the following conclusions can be drawn.

Based on the properties of cross wavelet transform, wavelet phase difference and linear time invariant systems theory, the following methodology is proposed to diagnose the source(s) of oscillation in a control loop.

- **Valve stiction**: If the oscillating source is only due to valve stiction, the cross wavelet transform plots should not only exhibit harmonics but also discontinuities.
- **Model plant mismatch:** If the source is due to model plant mismatch, which among the gain, time constant and delay causes the oscillation needs to be pinpointed.
  Gain mismatch: Gain mismatch theoretically does not affect the wavelet phase spectrum. Hence, the phase difference between $W_{uy}(f,\tau)$ and $W_{uy_m}(f,\tau)$ is zero at the fundamental frequency of oscillation. Cross wavelet spectrum ratio is constant at non-zero value at the frequency of oscillation. Further, the average phase angles of $W_{uy}(f,\tau)$ and $W_{uy_m}(f,\tau)$ estimated at the frequency of oscillation are theoretically same. In addition to this, the arrows in cross wavelet transform plots will be in same direction.
  Time constant mismatch: Time constant mismatch affects both cross wavelet spectrum ratio and phase spectrum. The plots of both $\frac{|W_{uy}(f,\tau)|}{|W_{uy_m}(f,\tau)|}$ and $\phi_{uy}(f,\tau) - \phi_{uy_m}(f,\tau)$ clearly show that the time constant mismatch significantly changes behavior of absolute cross wavelet spectrum ratio and the phase spectrum. Consequently, the average phase angles of $W_{uy}(f,\tau)$ and $W_{uy_m}(f,\tau)$ estimated at the frequency of oscillation are different. The arrows in cross wavelet transform plots will be in same direction since the effect of time constant mismatch on phase spectrum is minimum.
  Delay mismatch: Delay mismatch theoretically does not affect the magnitude of cross wavelet phase spectrum. Hence, cross wavelet spectrum ratio is unity at the frequency of oscillation. In contrast, the phase difference between $W_{uy}(f,\tau)$ and $W_{uy_m}(f,\tau)$ is non-zero at the fundamental frequency of oscillation and the average phase angles of $W_{uy}(f,\tau)$ and $W_{uy_m}(f,\tau)$ estimated at the frequency of oscillation are different. Consequently, the arrows in cross wavelet transform plots will be in opposite direction.

4. SIMULATIONS

A control system consisting of a process characterized by the transfer function $G_p = \frac{K_p}{\tau_p s+1}e^{-d_p s}$and model $G_m = \frac{K_m}{\tau_m s+1}e^{-d_m s}$ is simulated with IMC controller for a unit step change in the set point. The different

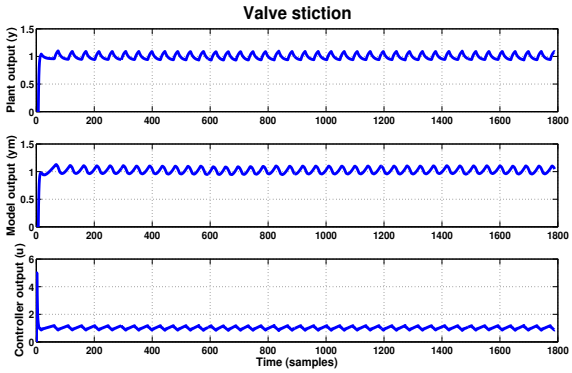

Fig. 4. Time domain behavior of plant, model and controller outputs for the valve stiction as the source of oscillation.

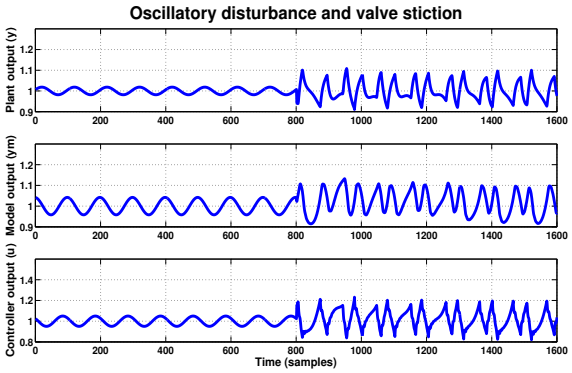

Fig. 5. Time domain behavior of plant, model and controller outputs for the case oscillatory output and valve stiction as the sources of oscillation

case studies analyzed for the diagnosis of oscillation in a control loop are (*i*) oscillation due to valve stiction (*ii*) oscillation due to valve stiction and oscillatory disturbance (*iii*) oscillation due to gain mismatch (*iv*) oscillation due to gain mismatch and oscillatory disturbance and (v) oscillation due to delay mismatch.

4.1 Diagnosis of valve stiction

A simple yet efficient one parameter model proposed by (Hägglund 1995) is used to generate oscillations due to valve stiction. The model is

$$x(t) = \begin{cases} x(t-1) & |u(t) - x(t-1)| \leq d \\ u(t) & \text{otherwise} \end{cases} \quad (6)$$

Here $u(t)$ and $x(t-1)$ are present and past valve outputs, $u(t)$ is the present controller output, and d is the valve stiction band. The valve stiction band is expressed in terms of the percentage or fraction of valve movement corresponding to the amount of stiction present in the valve. For instance, if 100 units of force are required to open the valve completely from completely closed position and 10 units of force is required to overcome the amount of static friction in the valve, stiction band is 10% or 0.1. The stiction band of 0.1 is used in the simulation. Model plant mismatch is introduced by changing the values of gain, time constant and delay appropriately in the process. The sinusoidal disturbance of frequency 0.01 Hz is considered for the simulation.

The cross wavelet transform computed between controller output and plant output is compared with that computed between controller output and model output. In the case of oscillation due to valve stiction (Figure 4), the plots of cross wavelet transform (Figures 6 & 7) not only show harmonics but also discontinuities which are the characteristics of a sticky valve. Figures 8 and 9 clearly indicate the presence of the valve stiction as one of the sources of oscillation between 800 and 1600 s and the other being the oscillatory component of frequency 0.01 Hz throughout.

4.2 Gain mismatch

If the oscillation is only due to MPM, there will be clearly a single frequency in the cross wavelet transform plot. The

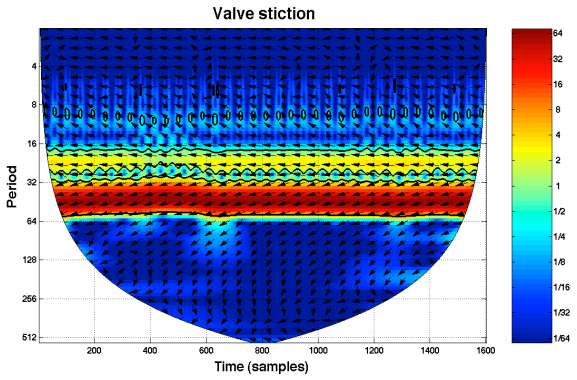

Fig. 6. Cross wavelet transform plot between u and y_p when the oscillation is only due to valve stiction.

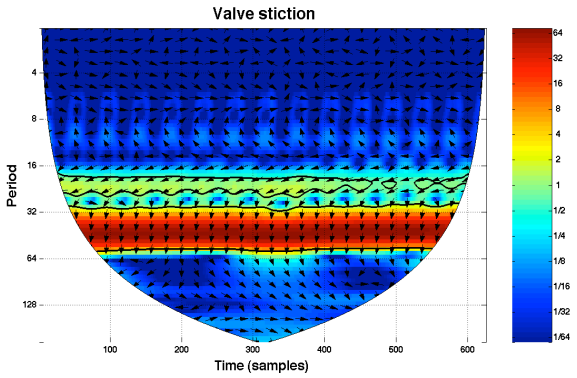

Fig. 7. Cross wavelet transform plot between u and y_m when the oscillation is only due to valve stiction.

system is simulated to generate oscillation in the plant output due to gain mismatch (Figure 10). The cross wavelet transforms, $W_{uy}(f,\tau)$ and $W_{uy_m}(f,\tau)$ are estimated from where the quantities, absolute cross wavelet transform ratio $\frac{|W_{uy}(f,\tau)|}{|W_{uy_m}(f,\tau)|}$, the phase difference, $\phi_{uy}(f,\tau) - \phi_{uy_m}(f,\tau)$ and average phase angles of $W_{uy}(f,\tau)$ and $W_{uy_m}(f,\tau)$ at the frequency of oscillation are obtained. The value of $\frac{|W_{uy}(f,\tau)|}{|W_{uy_m}(f,\tau)|}$ is found constant at 2.4 (Figure 13), the phase difference is zero (Figure 14) at the frequency of oscillation and the average phase angles are -2.551 and -2.554. The plots of $W_{uy}(f,\tau)$ and $W_{uy_m}(f,\tau)$ (Figures 11 & 12) show

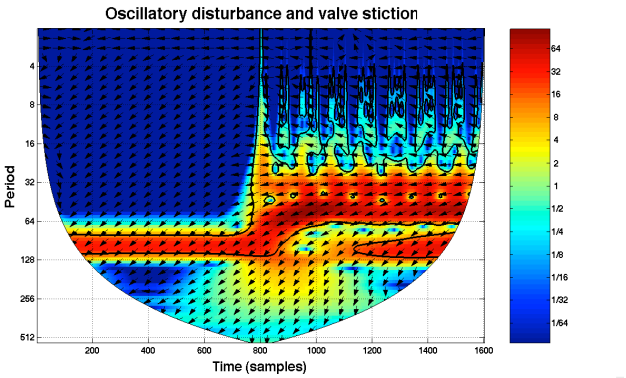

Fig. 8. Cross wavelet transform plot between u and y_p when the oscillation is due to oscillatory disturbance and valve stiction.

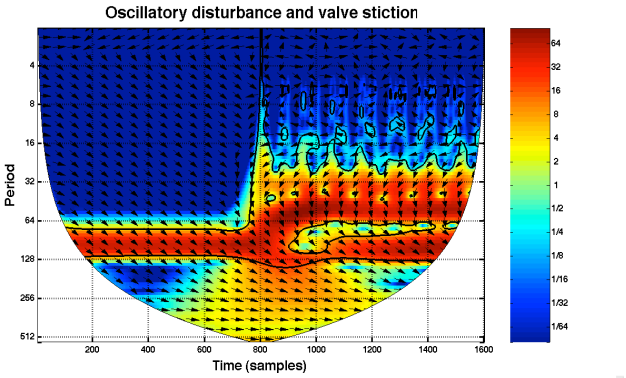

Fig. 9. Cross wavelet transform plot between u and y_m when the oscillation is due to oscillatory disturbance and valve stiction.

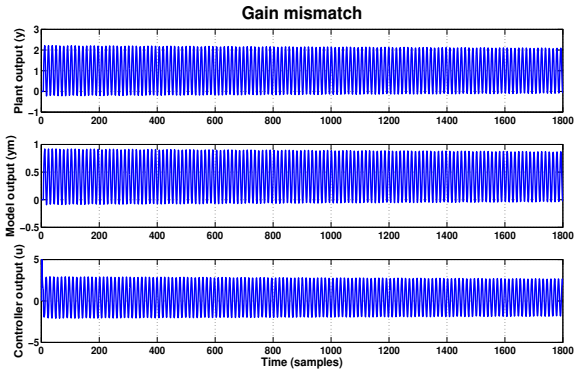

Fig. 10. Time domain behavior of plant, model and controller outputs for the case of gain mismatch as the source of oscillation.

that the arrows are in same direction. This is also in line with the fact that the phase spectrum is unaffected by the changes in gain.

4.3 Time constant mismatch

The control loop whose outputs are given in Figure (15) is analyzed for diagnosing the source(s) of oscillations. Figures (18) and (19) indicate the presence of time constant mismatch as the source of oscillation. Further, the

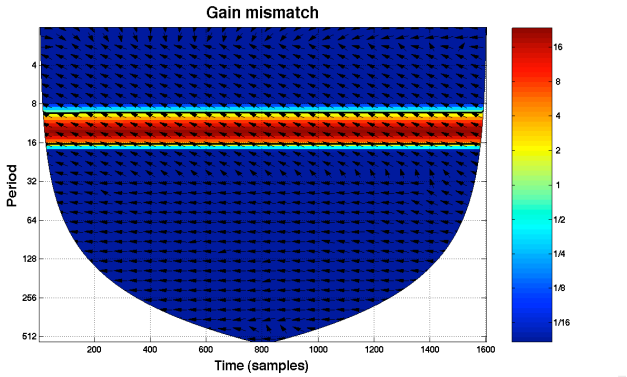

Fig. 11. Cross wavelet transform plot between u and y_p when the oscillation is gain mismatch

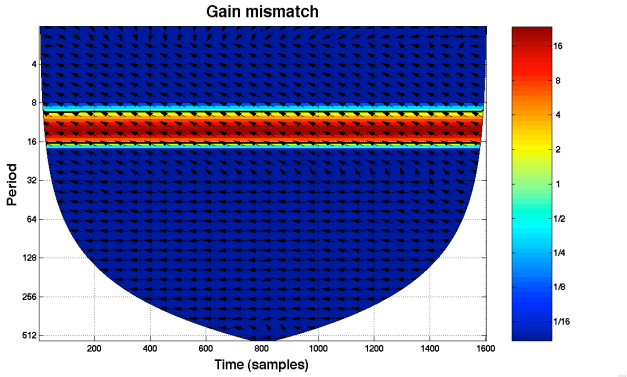

Fig. 12. Cross wavelet transform plot between u and y_m when the oscillation is gain mismatch

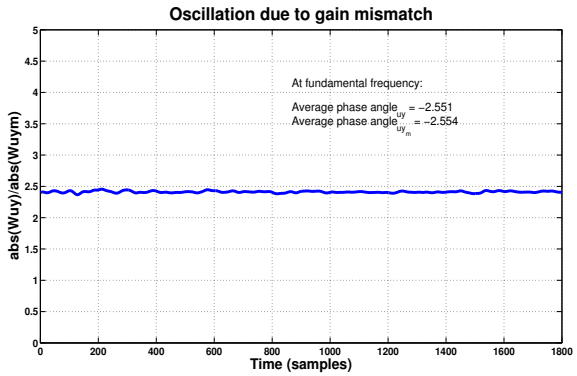

Fig. 13. A plot of ratio of cross wavelet transforms when the oscillation is due to gain mismatch.

closeness of the values of average phases angles (-2.4244 and -2.1488) strengthens the presence of time constant mismatch. Figures (16) and (17) indicate that the arrows are in the same direction. This is also expected in the case of time constant mismatch as the source of oscillation since the effect of time constant mismatch on phase spectrum is minimal.

4.4 Oscillation due to delay mismatch

The control loop whose outputs are given in Figure 20 is analyzed for diagnosing the source(s) of oscillations. The cross wavelet transforms, $W_{uy}(f,\tau)$ and $W_{uy_m}(f,\tau)$

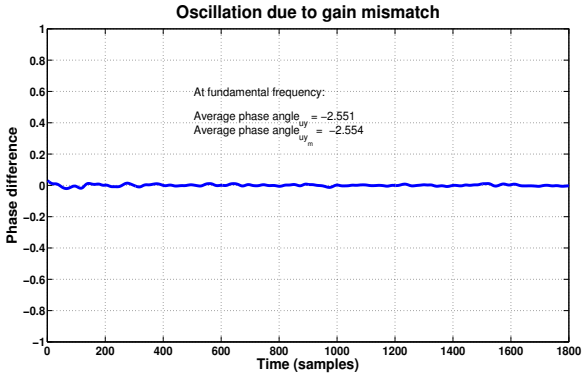

Fig. 14. A plot of phase difference when the oscillation is due to gain mismatch

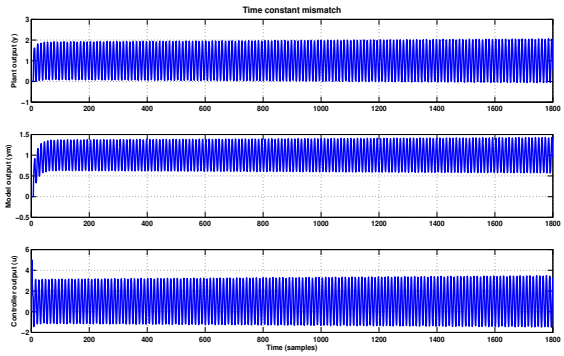

Fig. 15. Time domain plots of plant, model and controller outputs for the case of time constant mismatch as the source of oscillation

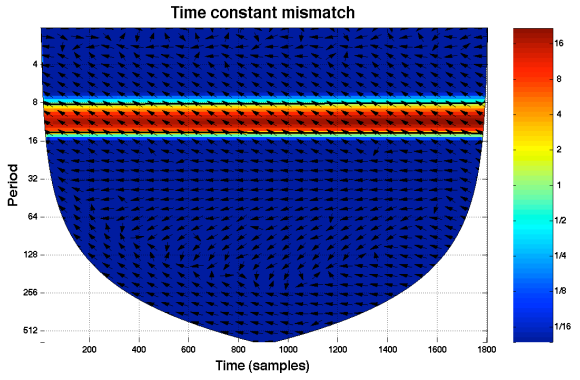

Fig. 16. Cross wavelet transform plot between u and y_p when the oscillation is due to time constant mismatch

are estimated from where the quantities, absolute cross wavelet transform ratio $\frac{|W_{uy}(f,\tau)|}{|W_{uy_m}(f,\tau)|}$, the phase difference, $\phi_{uy}(f,\tau) - \phi_{uy_m}(f,\tau)$ and average phase angles of $W_{uy}(f,\tau)$ and $W_{uy_m}(f,\tau)$ at the frequency of oscillation are obtained. The value of $\frac{|W_{uy}(f,\tau)|}{|W_{uy_m}(f,\tau)|}$ is found unity (Figure 23), the phase difference is non-zero (Figure 24) at the frequency of oscillation and the average phase angles are -2.9498 and 1.751. These observations show the presence of delay mismatch. Further, the plots of $W_{uy}(f,\tau)$ and $W_{uy_m}(f,\tau)$ (Figures 21 & 22) indicate that the arrows are

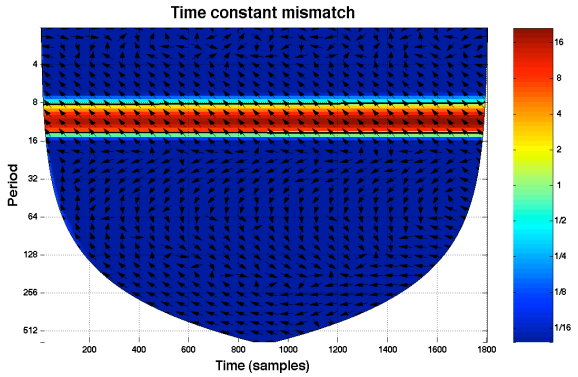

Fig. 17. Cross wavelet transform plot between u and y_m when the oscillation is due to time constant mismatch

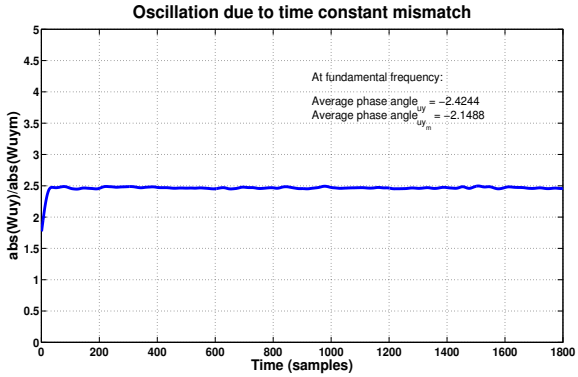

Fig. 18. A plot of ratio of cross wavelet transforms when the oscillation is due to time constant mismatch

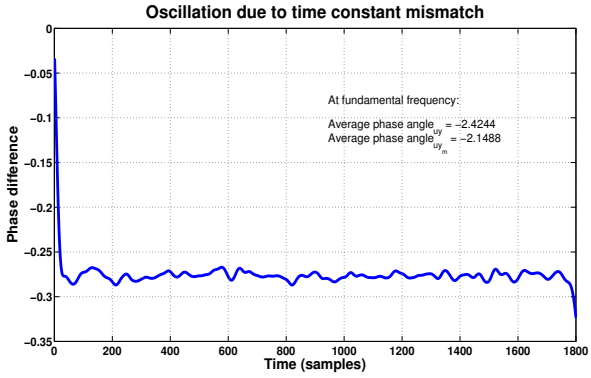

Fig. 19. A plot of phase difference when the oscillation is due to time constant mismatch

in opposite direction strengthening the presence of delay mismatch as the source of oscillation.

5. CONCLUSIONS

A pattern recognition technique combined with two key measures namely, absolute cross wavelet transform ratio and wavelet phase difference for the diagnosis of control loop oscillations in internal model control systems due to multiple sources has been developed. A diagnostic study of oscillation due to either one of valve stiction, model plant mismatch, oscillatory disturbance or combination of these has been presented. The oscillations due to valve stiction manifest as harmonics as well as discontinuities

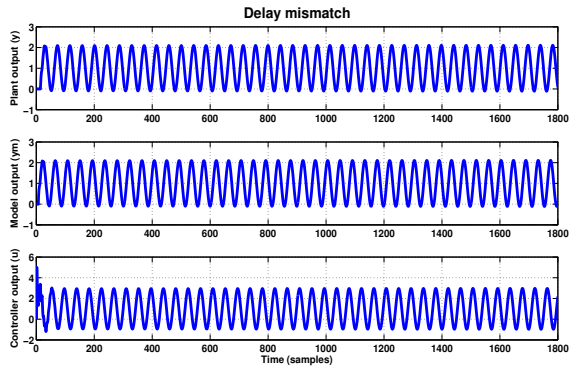

Fig. 20. Time domain plots of plant, model and controller outputs for the case of delay mismatch as the source of oscillation.

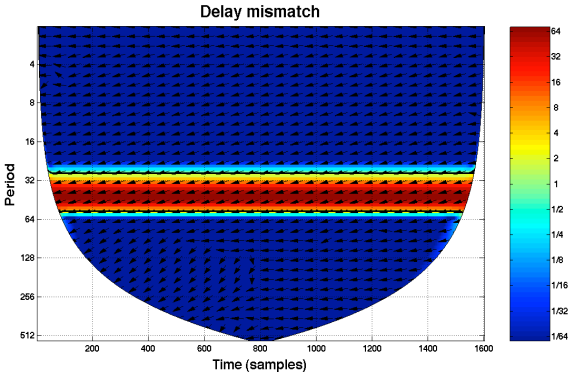

Fig. 21. Cross wavelet transform plot between u and y_p when the oscillation is due delay mismatch..

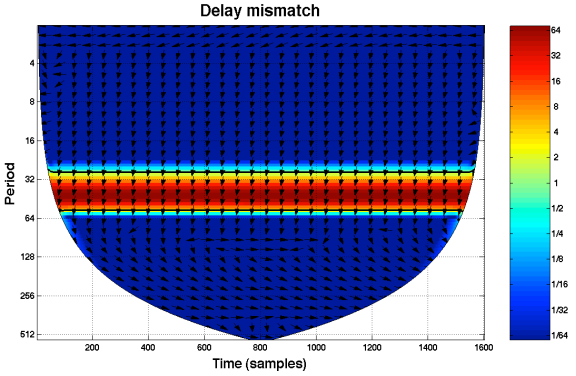

Fig. 22. Cross wavelet transform plot between u and y_m when the oscillation is due delay mismatch..

in the cross wavelet transform plots whereas oscillation due to model plant mismatch leaves distinct signatures in the phase information (arrows). If the oscillations are due to gain mismatch, the absolute cross wavelet transform is constant at non-zero value at the frequency of oscillation and the wavelet phase difference is zero. Further, the plots of $W_{uy}(f,\tau)$ and $W_{uy_m}(f,\tau)$ show the arrows are in same direction which strengthens the finding of the gain mismatch as the source of oscillation. If the oscillation is due to time constant mismatch, both the quantities, the absolute cross wavelet transform and the the wavelet phase difference are affected. On the other hand, oscillation due

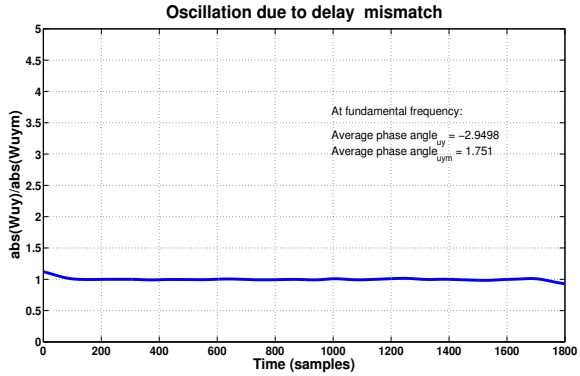

Fig. 23. A plot of ratio of cross wavelet transforms when the oscillation is due to delay constant mismatch

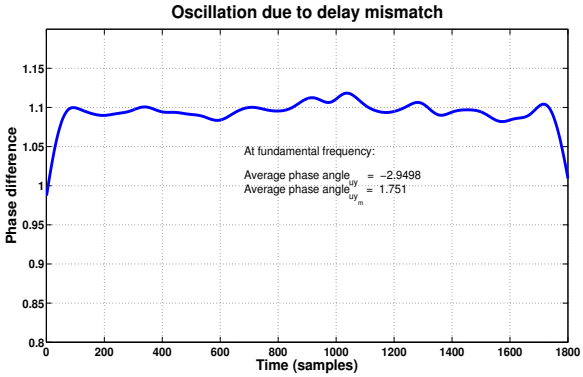

Fig. 24. A plot of phase difference when the oscillation is due to delay mismatch

to delay mismatch results in a directional change in the phase difference while the absolute cross wavelet transform ratio is unity at the frequency of oscillation.

REFERENCES

Bloomfield, D.S., R.T.J. McAteer, B.W. Lites and P.G. Judge (2004). Wavelet phase coherence analysis: Application to a quiet-sun magnetic element. *The Astrophysical Journal* **617**, 623–632.

Choudhury, M.A.A.S., S.L. Shah and N.F. Thornhill (2004). Detection and quantification of control valve stiction. In: *DYCOPS*. Boston, USA.

Forsman, K. and A. Stattin (1999). A new criterion for detecting oscillations in control loops. In: *CP8-3*. European control conference. Karlsruhe, Germany.

Hägglund, T. (1995). A control-loop performance monitor. *Control Engineering Practice* **3**, 1543–1551.

Horch, A. (1999). A simple method for the detection of stiction in control valves. *Control Engineering Practice* **7**, 1221–1231.

Horch, A. and A.J. Isaksson (1998). A method for detection of stiction in control valves. In: *Online fault detection and supervision in the chemical process industry*. IFAC Workshop. Lyon, France. p. 4B.

Rengaswamy, R., T. Hägglund and V. Venkatasubramanian (2001). A qualitative shape analysis formalism for monitoring control loop performance. *Engineering Applications of Artificial Intelligence* **14**, 23–33.

Tangirala, A.K., J. Kanodia and S.L. Shah (2007). Non negative matrix factorization for detection and diag-

nosis of plant wide oscillations. *Industrial & Engineering Chemistry Research* **46**, 801–817.

Thornhill, N.F. and T. Hägglund (1997). Detection and diagnosis of oscillation in control loops. *Control Engineering Practice* **5**, 1343–1354.

Thornhill, N.F., B. Huang and H. Zhang (2003). Detection of multiple oscillations in control loops. *Journal of Process Control* **13**, 91–100.

Torrence, C. and G.P. Compo (1998). A practical guide to wavelet analysis. *Bulletin of the American Meteorological Society* **79**, 61–78.